Chinese Chemical Letters 33 (2022) 22–32

Contents lists available at ScienceDirect

Chinese Chemical Letters

journal homepage: www.elsevier.com/locate/cclet

Recent advances in nanoscale metal-organic frameworks biosensors for detection of biomarkers

Qiu-Yang Xu[a], Zheng Tan[a], Xue-Wei Liao[b,*], Chen Wang[a,c,**]

[a] Department of Chemistry, China Pharmaceutical University, Nanjing 211198, China
[b] Analytical and Testing Center, Nanjing Normal University, Nanjing 210046, China
[c] Jiangsu Key Laboratory of New Power Batteries, School of Chemistry and Materials Science, Nanjing Normal University, Nanjing 210023, China

ARTICLE INFO

Article history:
Received 28 February 2021
Revised 26 April 2021
Accepted 6 June 2021
Available online 11 June 2021

Keywords:
Nanoscale metal-organic frameworks
Biosensors
Biomarkers
Nano-platforms
Early diagnosis

ABSTRACT

Early and precise diagnosis are propitious to timely treatment and simultaneously increase the chance of successful treatments. It is of critical importance to develop rapid, sensitive, and reliable sensing techniques of physiological biomarkers for disease diagnosis. Due to the advantages of structural designability and property tunability, nanoscale metal-organic frameworks (nMOFs) have been widely applied in the field of biomedicine in recent years. Particularly, enhanced stability, more modification sites and improved distribution make nMOFs more suitable as biosensors for detection of biomarkers. This review article will summarize the recent advancements of nMOFs-based biosensors for detection of biomarkers, classified into four sections *via* different sensing modes: fluorescent sensing, colorimetric sensing, electrochemical sensing and surface-enhanced Raman scattering (SERS) sensing within the latest years. Except introducing and comparing the role of nMOFs in different sensing modes, designing strategies of nMOFs-based biosensors are involved as well. At last, a brief conclusion and outlook for further applications are provided, which is helpful for exploring multi-functional biologic nano-platforms with nMOFs. We expect that this review can inspire the interest on this promising research area of nMOFs-based biosensors for detection of biomarker and early diagnosis.

1. Introduction

The stable contents of physiological species (such as ions, small molecules, nucleic acids and proteins) are significant to cellular functions and normal physiological activities. The variations of physiological species on concentrations or types would indicate the metabolic disorders or pathological disturbances. Early and precise diagnosis through qualitatively or quantitatively detecting of physiological biomarkers are propitious to timely treatment and increase the chance of successful treatments [1,2]. A number of biosensing methods including lateral flow immunoassay [3], polymerase chain reaction (PCR) [4] and enzyme-linked immunosorbent assay (ELISA) have been widely used in clinical diagnosis [5]. Compared with these conventional methods, it is expected to develop convenient, rapid and inexpensive biosensors with high sensitivity and selectivity for monitoring biomarkers in real-time.

Biosensors are sensing devices used to analyze organic or inorganic molecules *in vitro* or *in vivo*, composing of biological receptor and physicochemical transducer [6]. According to the different types of the contained bioreceptors, biosensors are divided into enzymatic sensors, nucleic acid sensors, cell sensors, biomimetic sensors and so on. Owing to the rapidly promoted sensitivity and selectivity, these biosensors have widely used in various fields such as biomedicine [7,8], environmental [9] and agri-food safety [10,11]. In recent years, with the rapid development of nanotechnology, novel biosensors based on different nanomaterials have been continuously explored including carbon nanotubes [12], carbon dots [13], graphene oxide (GO) [14], molybdenum disulfide (MoS_2) nanosheets [15], gold nanoparticles (AuNPs) [16–18], hydrogels [19], anodic aluminum oxide (AAO) [20–22], metal-organic frameworks (MOFs) [23–25] *etc*. They have not only shown good sensitivity and affinity to biomolecules, but also protected bioreceptors form environmental damage, making diagnosis more effectively and promptly at the molecular and cellular level.

* Corresponding author.
** Corresponding author at: Department of Chemistry, China Pharmaceutical University, Nanjing 211198, China.
E-mail addresses: liaoxuewei@njnu.edu.cn (X.-W. Liao), wangchen@njnu.edu.cn (C. Wang).

https://doi.org/10.1016/j.cclet.2021.06.015
1001-8417/

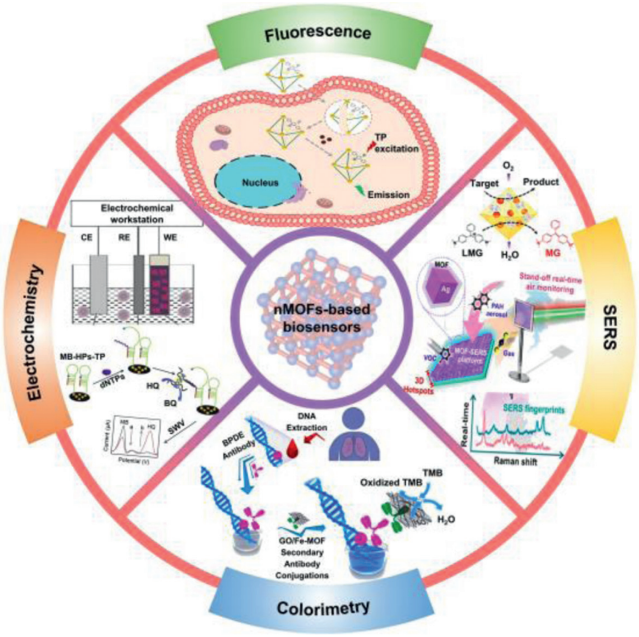

Fig. 1. Detection methods of biomarkers using nMOFs biosensors *via* four sensing technologies: fluorescence, colorimetry, electrochemistry and SERS.

Among them, MOFs stood out. As an emerging class of crystalline porous compounds consisted of metal-containing nodes (known as secondary building units, SBUs) and organic linkers, MOFs integrate the advantages of both organic and inorganic materials [26]. Due to the extraordinarily high surface areas, structural and property tunability, MOFs have rapidly developed in numerous fields. Designing unique porous environment or crystal defects in MOFs improved the performance for gas separation [27] and electrocatalysis [28]. In addition, MOFs have also played important roles in fuel cells [29], energy conversion [30,31], catalysis [32,33] and chemical sensors [34]. Especially, nanoscale metal-organic frameworks (nMOFs) with enhanced chemical/colloidal stability, more effective surface modification sites and improved biological distribution, are more considerable for varied applications [35]. There are three outstanding advantages for nMOFs biosensors. First, the highly ordered pores and large specific surface area improve the loading rate of functional agents for sensing. Second, the structures of nMOFs are various and designable by changing the functional nodes or linkers, which will endow the nMOFs with special functions. Third, the biosafety can be ensured by selecting biocompatible molecules as parts of nMOFs. Therefore, nMOFs have been become more dramatic and beneficial alternative biosensors with superior analytical performance including high sensitivity, good repeatability, and low detection limit. In recent years, there is a growing interest in developing nMOFs biosensors for detection of various biomarkers and early diagnosis. An updated review with recent advances in this field is highly desired.

In this review, we will focus on the advances in nMOFs biosensors for biomarkers detection in recent five years. In accordance with different analytical technologies, biomarkers are determined or even quantified using nMOFs-based biosensors *via* fluorescence, colorimetry, electrochemistry and surface-enhanced Raman scattering (SERS) (Fig. 1). Impressively, the comparisons of the roles of nMOFs in different sensing modes and designing strategies of nMOFs biosensors will be demonstrated as well. Moreover, the prospects and key challenges in this area will be discussed. This review is intended to promote the awareness of current developments of nMOFs biosensors and their potential applications in sensing and monitoring of biomarkers. We expect that this review can highlight the superiority of multifunctional nMOFs in various analytic methods and inspire the nanomaterials community to think about possible clinical applications of nMOFs-based biosensors for early diagnosis.

2. Fluorescent sensing

It is well known that fluorescence is one of most popular detection methods with excellent analytical performance such as high sensitivity, selectivity and real-time response capability [36–38]. Based on the distance-dependent fluorescence resonance energy transfer (FRET), photoinduced electron transfer (PET) or other quenching mechanisms through fluorophore-quencher pairs, various nMOFs-based fluorescent nanoprobes have been designed as biosensors [39]. NMOFs can respond to the interactions between the inserted guest species and framework through different degrees of luminescence enhancement or quenching, exhibiting excellent molecular recognition and signal transduction [40]. In fluorescent nanoplatforms, nMOFs can act as fluorophores, fluorescence quenchers or skeletons. Although nMOFs exhibit different functions, they all play very important roles in the fluorescent biosensing process.

2.1. NMOFs as fluorophores

Most of the inherent fluorescence of luminescent metal-organic frameworks (LMOFs) originate from ligand molecules, such as the aromatics or other conjugated linkers. Responsive signals based on the change in the fluorescence intensity, including luminescence quenching or enhancement, is defined as "turn-off" and "turn-on" responses, respectively. "Turn-off" fluorescent biosensing would be directly realized by the fluorescence quenching of LMOFs. For example, the miRNA-155 expression level was detected using a "sandwich-type" fluorescent biosensor (Fig. 2a) [41]. The La(III)-MOF and silver nanoparticles (AgNPs) were used as the energy donor-acceptor pairs. The target analyte would lead to the hybridization of oligonucleotides and quench the fluorescence through FRET process. This "turn-off" fluorescent biosensor could determine miRNA-155 as low as 5.5 fmol/L. Besides, xanthine oxidase (XO) activity was determined by a Zr-based MOFs named BTB-MOF with stable photoluminescence in both pure water and buffer solution [42]. The fluorescence emission of BTB-MOF induced by ligand-centered electron transition could be quenched by xanthine (the substrate of XO) and uric acid (the product of xanthine oxidation). Taking advantage of different quenching efficiency between xanthine and uric acid, BTB-MOF as a biosensor converted XO activity into changes of fluorescence signal intensity with good selectivity and low limit of detection (LOD) (0.004 U/L) in very short time (~1 min).

Compared with the "turn-off" fluorescence probes, it's easier to identify signals and avoid false positives under dark background for the "turn-on" probes. As typical example, a novel Zr-MOFs was synthesized as "turn-on" fluorescence probe for real-time detecting H_2S and S^{2-} with LOD of 1 ppb [43]. The N-S bond formed between H_2S and ligand tetrakis(4-carboxyphenyl)porphyrin (TCPP) was the key of "turn-on" strategy, leading to high selectivity of sensing H_2S. In addition, a simple "turn-on" fluorescence ascorbic acid (AA) biosensor based on the redox reaction in cerium MOFs was developed [44]. Ce^{4+} in MOFs would oxidize AA to dehydroascorbic acid with strong electron-withdrawing property, which could prevent the PET process from ligands to Ce ions and therefore enhance the fluorescence intensity. Furthermore, a "turn-on" dipicolinic acid (DPA) biosensor was also designed on account of the structural transformation of Eu-MOF (Fig. 2b) [45]. Through

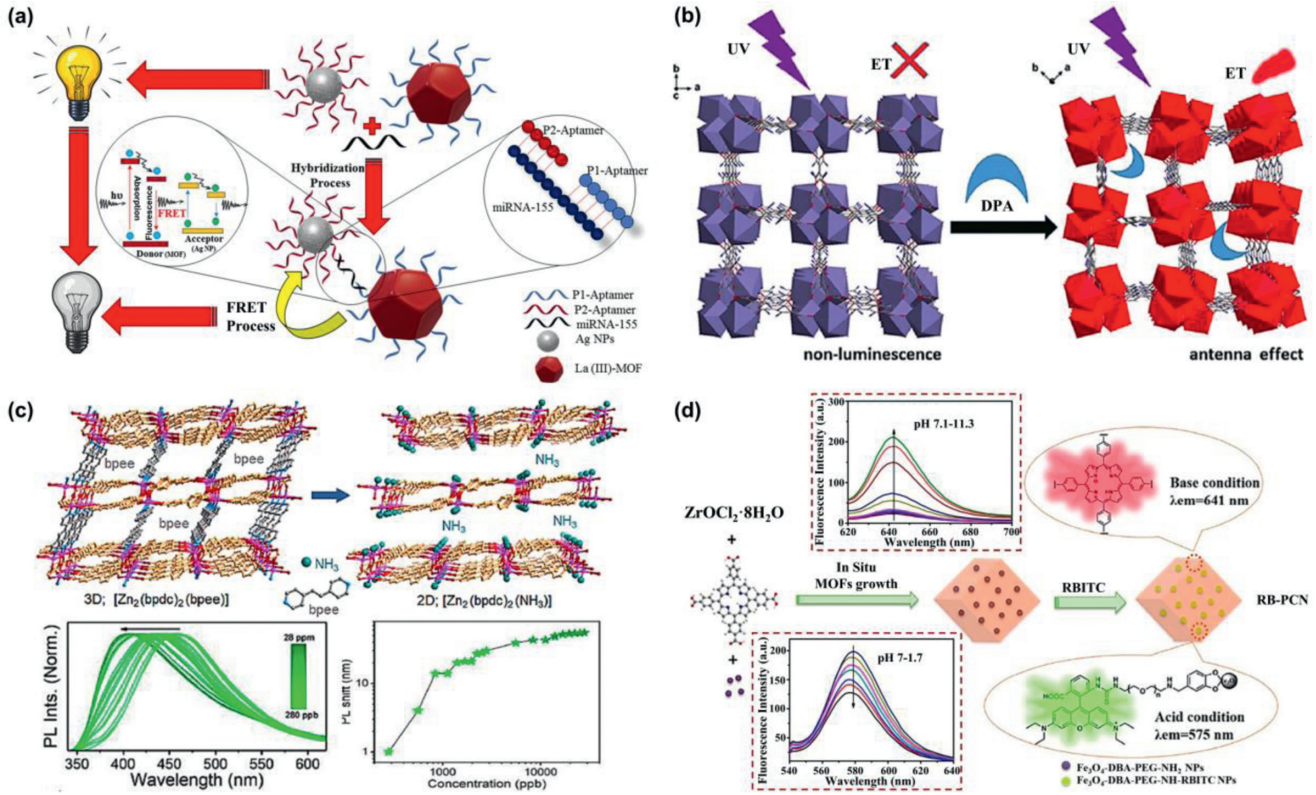

Fig. 2. (a) Schematic diagram of photoluminescence quenching-based detection of miRNA-155 as a cancer biomarker by the FRET process. Reproduced with permission [41]. Copyright 2020, American Chemical Society. (b) The as-formed 3D frameworks along the [001] direction and the response property for DPA. ET = energy transfer. Reproduced with permission [45] Copyright 2019, The Royal Society of Chemistry. (c) Schematic representation of the 2D structure potentially obtained after the NH_3 detection, PL spectra in aqueous solutions of NH_3 with different concentrations and magnitude of the 320 nm photoexcited PL peak shift as a function of NH_3 concentration. Reproduced with permission [46]. Copyright 2019, American Chemical Society. (d) Design strategy and fluorescence changes of RB-PCN upon pH variation and fluorescence spectra (λ_{ex} = 520 nm) of RB-PCN in acidic/basic aqueous solution. Reproduced with permission [48]. Copyright 2018, American Chemical Society.

the single-crystal to single-crystal phase transition, the luminescence properties were selectively restored by DPA with about 10^5 enhancement. Besides, the exchange between ligands and analyte amines would trigger the luminescence features of LMOFs which could be exploited for highly sensitive amine recognition with sub-ppm content (Fig. 2c) [46]. In another example, a recyclable MOFs-based test paper was prepared for the rapid detection of health indicators such as cysteine and glutathione [47]. The fluorescence of molecular vise PCN-521-isonicotinic acid (MV-MOF-IA) was quenched by Cu^{2+} in advance due to the ligand-metal charge transfer (LMCT). When the biomarker solution was added dropwise on test paper the fluorescence was recovered. The LODs were 22.5 nmol/L and 46.4 nmol/L for L-cysteine and glutathione, respectively. In order to monitor pH changes over a wide range in real-time, a nanocomposite probe with single excitation and dual emission fluorescence characteristics was synthesized (Fig. 2d) [48]. Rhodamine B isothiocyanates were covalently fixed in PCN-224 for fluorescence response to pH changes in acidic and alkaline environments, respectively. This nMOFs biosensor was conducive to H^+ shuttling and avoided the background interference as well.

According above-mentioned works, it can be seen that the biomarkers would be directly detected through straight triggering or quenching the fluorescence of luminescent nMOFs.

2.2. NMOFs as fluorescence quenchers

Fluorescence quenching caused by energy transfer including FRET, PET or other quenching mechanisms between fluorophores and nMOFs have been used for developing new biosensors. When nMOFs acts as fluorescent quenchers, the fluorescence intensity could be adjusted *via* blocking the energy transfer process or changing the distance between nMOFs and fluorophores. NMOFs are considered to be the promising materials to detect nucleic acid due to their high affinity with biomolecules through electrostatic, π-stacking, and hydrogen-bonding interactions. Zhang's group synthetized a two-dimensional (2D) Cu-TCPP nanosheet with fluorescence quenching ability, and used it as the fluorescence platform for DNA detection [49]. The TCPP ligand containing conjugated π-electron system allowed for the binding of single-stranded DNA (ssDNA), but has little affinity with double-stranded DNA (ds-DNA). Therefore, the detection of target DNA was performed utilizing this obvious adsorption distinction between different structures. Besides, the fluorescence signal would be significantly amplified through combining with the hybridization chain reaction (HCR) strategy, which further reduced the detection limit in living cells [50]. Subsequently, a 2D MOFs-based multicolor fluorescent aptamer nanoprobe was constructed for detecting multiple antibiotics quickly, sensitively, and selectively (Fig. 3a) [51]. The luminescence of fluorescent-dye-labeled ssDNA was quenched by 2D MOFs. When the adsorbed ssDNA formed double helix dsDNA, its fluorescence was almost fully recovered. Notably, the surface charge properties of nMOFs plays an important role in the fluorescence changes of different dye molecules. Xia's group found that during DNA sensing process the quenched fluorescence might be further quenched, and the fluorescence quenching behavior could be reversed by adjusting the negative or positive charged property of MIL-101 [52]. Inspired by these findings, they designed an ATP-aptamer/lanthanide-based MOFs nanosheet complex to monitor ATP activity in living cells [53]. The charge properties (positive or negative) of the labeled fluorophores determined the fluores-

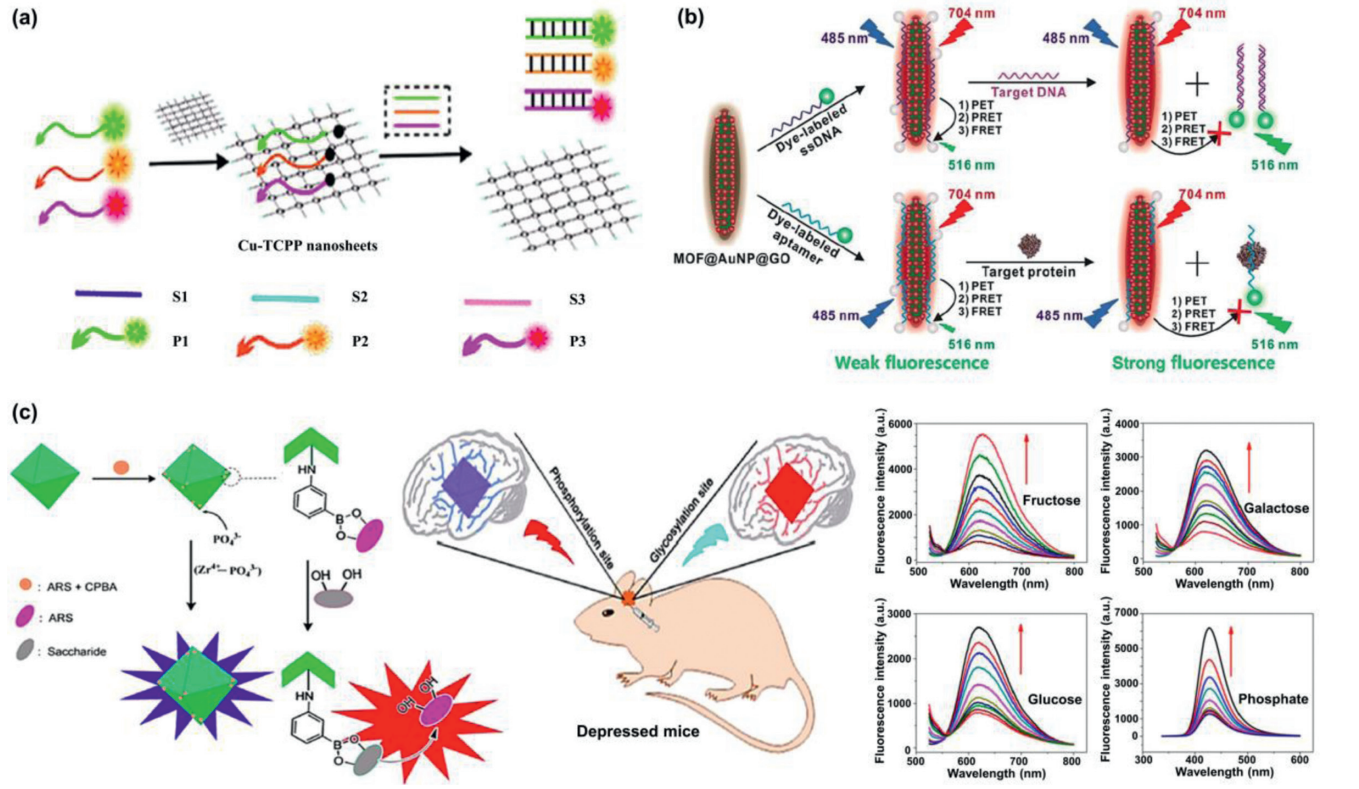

Fig. 3. (a) Schematic representation of detection of multiple antibiotics based on 2D Cu-TCPP Nanosheets. Reproduced with permission [51]. Copyright 2019, American Chemical Society. (b) Schematic diagrams for fluorescence recovery-based ratiometric no-wash biosensor for target DNA and protein detection by using MOF@AuNP@GO as synergistic nanoquencher. Reproduced with permission [54]. Copyright 2018, Ivyspring International Publisher. (c) Proposed mechanism of the fluorescence probe for detection of the levels of glycosylation and phosphorylation based on Zr(IV)-MOF nanomaterials, *in situ* fluorescence imaging of the levels of glycosylation and phosphorylation in depressed mice and fluorescence response of MOF nanoprobe with fructose, galactose, glucose and phosphate solution, respectively. Reproduced with permission [57]. Copyright 2020, American Chemical Society.

cence quenching or recovery on MOFs nanosheets. Accordingly, an excellent two-color sensing platform for the intracellular detection was realized based on the Ln-MOF nanosheets with interesting fluorescence quenching properties.

Nevertheless, pure MOFs-based nanoquenchers present insufficient fluorescence quenching efficiency towards dye molecules, which may lead to the relative lower detection sensitivity. Designing new MOFs nanostructures with higher fluorescence quenching ability is thus of great significance to decrease background noise signal and increase the detection sensitivity. Chen's group designed a "three-in-one" nanohybrid as synergistic quencher for cancer biomarker detection with high-sensitivity (Fig. 3b) [54]. The proposed nanohybrid, MOF@AuNP@GO, consists of three common quenching nanomaterials, including Zr-based MOF, AuNPs and GO for quenching *via* PET, plasmonic resonance energy transfer (PRET) and FRET, respectively. Based on the similar principle, lanthanide ions were doped into zeolitic imidazolate framework-8 (ZIF-8) to regulate its fluorescence quenching behavior. The charge transfer from fluorophores to lanthanum ions occurs, showing around 3 times higher signal-to-background ratio than pure ZIF-8 [55].

Except for nucleic acids, other nMOFs-based biomarker sensors have also been fabricated. For instance, H_2S was detected by a Cu-ZnTCPP fluorescent probe [56]. The fluorescence of ZnTCPP ligand was quenched by Cu(II) ions. When Cu(II) ions combined with H_2S through Cu-S coordination, frameworks decomposed itself and therefore the energy transfer process was blocked, leading to the fluorescence recovery of ZnTCPP ligand. In addition, a Zr(IV) nMOFs-based fluorescent probe was designed and prepared for simultaneous detection of glycosylation and phosphorylation level to explore the relationship between them (Fig. 3c) [57]. The fluorescence generated by the specific interaction between Zr metal center and phosphate enabled sensitive detection of phosphorylation levels. The rich boric acid group modified on MOFs could combine both fluorophore alizarin red and glycosyl, and the glycosylation level would be detected through the competition between alizarin red and glycosyl. This research was of great significance for studying mechanisms and early diagnosis of the disease.

In view of the significative works, nMOFs-based fluorescent quenchers have been displayed potentiality for further clinic detection of typical biomarkers.

2.3. NMOFs as skeletons

As a class of nanomaterials with high porosity, nMOFs are able to support a large number of fluorophores with high loading rate. On the basis of this outstanding advantage, Li's group prepared functionalized nMOFs nanoprobes for highly sensitive multicolor fluorescence detection of DNA (Fig. 4a) [58]. In their work, nMOFs served as a vessel carrying signal dyes, then covered by DNA hairpin structure to close the holes *via* steric effect. After introducing the target DNA, the competitive substitution reaction opened the hairpin structure and triggered the release of fluorophore within the nMOFs holes. Through designing different hairpin DNA gatekeepers according to target DNA and loading different signal molecules, multi-detection was realized. Furthermore, the application range could be extended to proteins and the like. Besides, degradable nMOFs could act as carriers for intracellular codelivery of fluorescence probes. As an example, a DNA@Cu-MOF nanosystem was rationally designed for deregulated miRNA-related hypoxic tumor diagnosis (Fig. 4b) [59]. The hypoxia environment

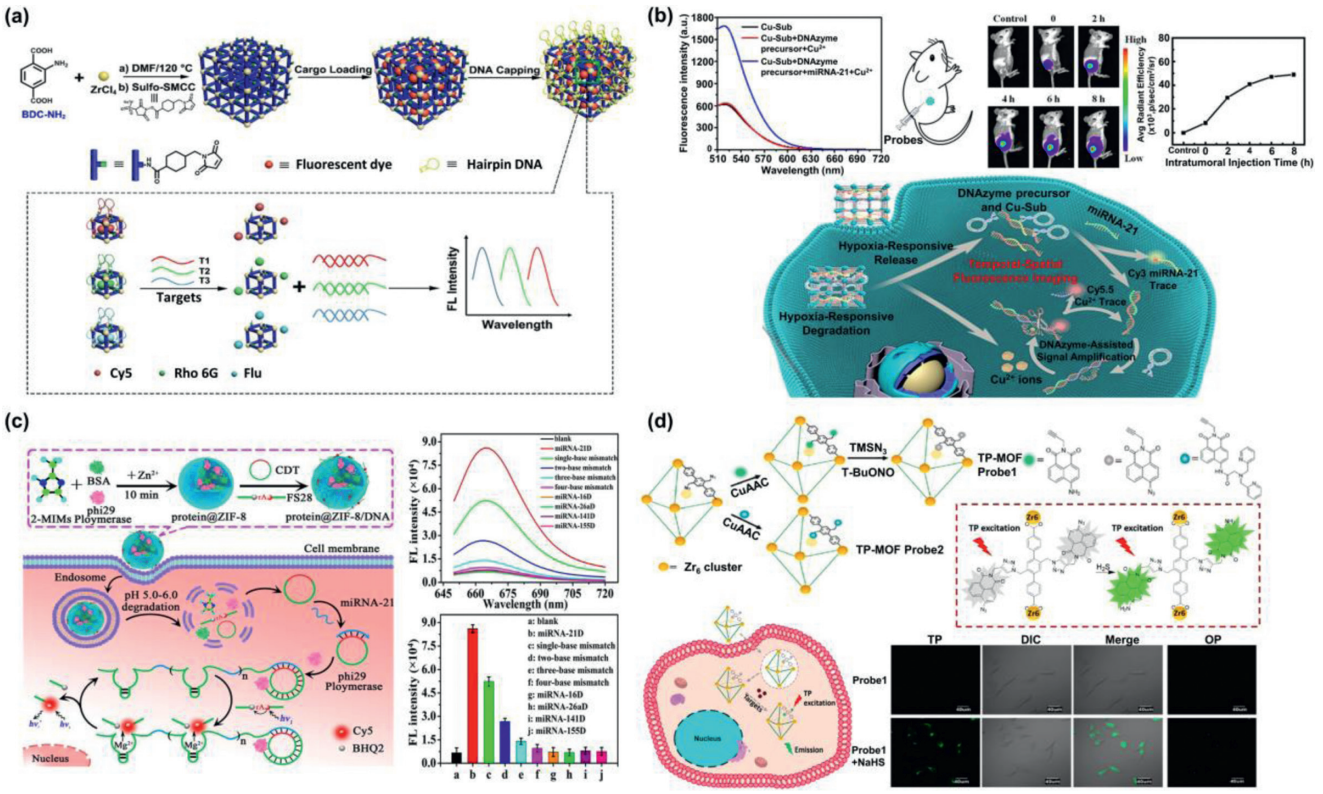

Fig. 4. (a) Schematic diagram for the fabrication process of MOF-based nanoprobes and multicolor detection of DNA targets. Reproduced with permission [58]. Copyright 2018, American Chemical Society. (b) Schematic illustration of hypoxia-responsive DNA@Cu-MOF nanoprobes for aberrant miRNA, detection of miRNA-21 *via* fluorescence intensities analysis, fluorescence images of MCF-7 tumor bearing mice treated with DNA@Cu-MOF nanoprobes with different time points and corresponding fluorescence intensity. Reproduced with permission [59]. Copyright 2020, American Chemical Society. (c) Illustration of microRNA-21 detection in living cells using ZIF-8 as a nanocarrier for codelivery of DNA probes, fluorescence spectra and fluorescence intensities in different DNA primers. Reproduced with permission [60]. Copyright 2019, American Chemical Society. (d) Schematic illustration for the construction of TP-MOF sensing platform and the process of intracellular sensing and confocal microscopy images of H_2S in HeLa cells. Reproduced with permission [61]. Copyright 2019, American Chemical Society.

induced the degradation of Cu-MOF and released signal strand. Target aberrant miRNA-21 displaced the signal strand through the toehold-mediated strand displacement hybridization followed by the fluorescence recovery of Cy3-labeled block DNA. In another example, a pH-sensitive biodegradable ZIF-8 was utilized as carrier system for intracellular delivery (Fig. 4c) [60]. After uptake into cells, the ZIF-8 was degraded and surface-adsorbed DNA probes were released, realized miRNA-21 monitoring in living cells.

Adjustable organic ligands also provide the possibility of covalently modifying fluorophores. Click chemistry technology was first used to prepare two-photon metal-organic framework (TP-MOF)-based fluorescence sensing platform (Fig. 4d) [61]. Azide-containing PCN-58 was the model building block and provided an enough cavity for fluorophores. Fluorescence of fluorophore was activated by H_2S or Zn^{2+} for sensing and intracellular imaging. The TP-MOF probe retained the fluorescence response characteristics of the organic linkers, and displayed excellent photostability, selectivity as well as biocompatibility.

In particular, the analytical performance of fluorescence detection could be affected by special functional groups of MOFs. For example, silver nanoclusters (AgNCs) were coated with ZIF-8 [62]. The "electron donor effect" of the nitrogen-containing ligands in MOFs greatly enhanced the fluorescence intensity of AgNCs, thus largely improving the sensing stability for biomolecules. This design not only combined the advantages of the two nanomaterials, but also provided new ideas for subsequent probe design. Therefore, nMOFs as skeletons or carriers of fluorescent molecules are functionalized media which is of great significance to the transmission and response of fluorescence signals.

As can be seen above, nMOFs-based fluorescent biosensors have successfully achieved the rapid or even real-time detection of biomarkers through changing the energy transfer process or structural transformation. Among design of biosensors, nMOFs played different roles including fluorophores, quenchers and skeletons. Although labeled molecules were needed, nMOFs exhibited multifunctions in fluorescence sensing system avoiding false positives, decreasing background noise signal and realizing the visualization.

3. Colorimetric sensing

Colorimetric sensing has attracted widespread attentions because the detection results are easily to read-out and fast to be visual determined *via* naked eyes or common instruments. As a mostly common case, the colorimetric sensing is realized using enzyme/nanozyme that catalyze the chromogenic substrates such as 3,3′,5,5′-tetramethylbenzidine (TMB), 2,2′-azino-bis(3-ethylbenzothiazoline-6-sulfonic acid) (ABTS) or *o*-phenylenediamine (OPD) into colorful products [63]. Based on the changed colors, a rapid, simple and inexpensive strategy for sensing could be provided.

3.1. NMOFs as nanozyme

Recently, the inherent enzyme-like catalytic activity of some nMOFs have been proven and the corresponding nMOFs biosensors have been developed. It is observed that multiple analytes can be detected by colorimetric sensing. For instance, a colorimetric sensor based on Ni-hemin MOFs nanozyme with highly peroxidase

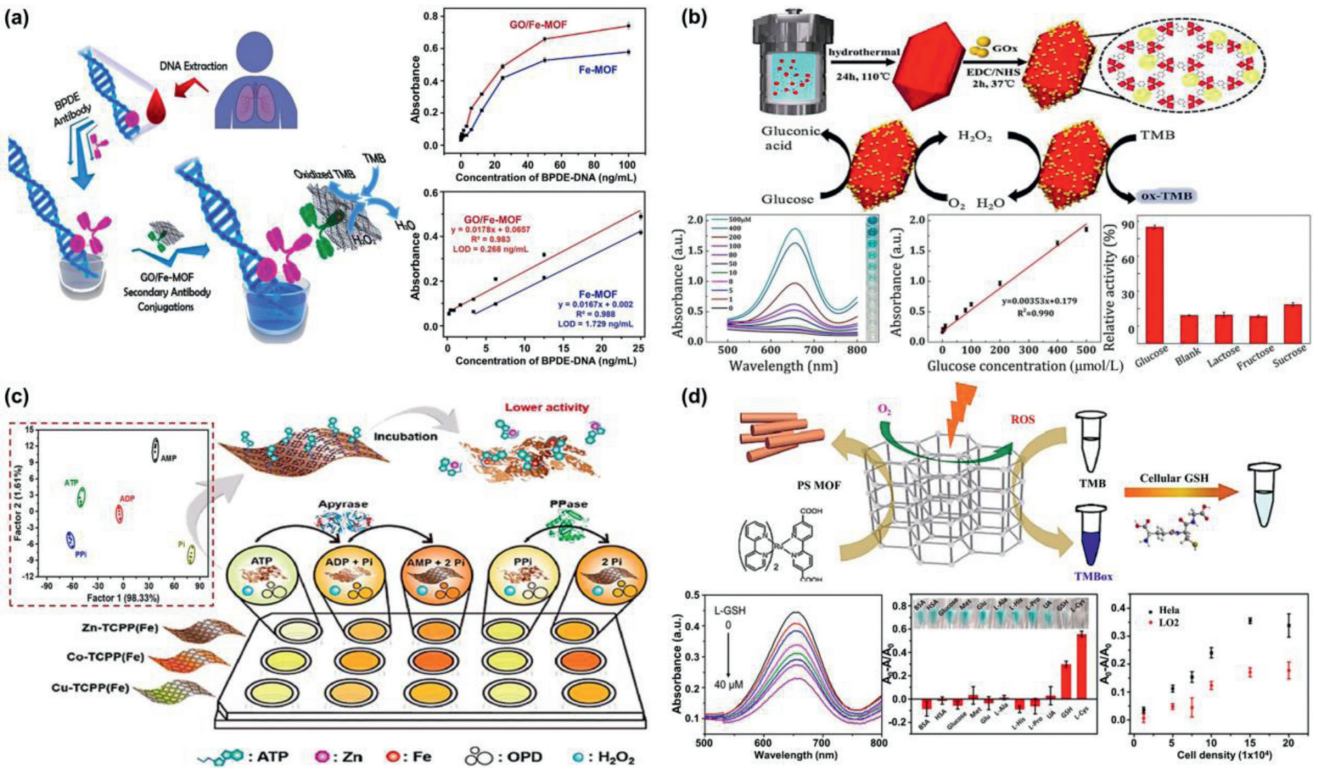

Fig. 5. (a) Ultrasensitive determination of the biomarker level in human blood through the bioamplification of the superior nanozyme, the standard curve for biomarker detection using Fe-MOF and GO/Fe-MOF nanozyme nest, respectively and corresponding linear calibration curves. Reproduced with permission [65]. Copyright 2019, American Chemical Society. (b) Schematic illustration of the synthetic approach of Fe-MOF-GOx and corresponding cascade catalytic detection of glucose, UV–vis spectra and digital photo (inset) of cascade reaction with series glucose concentration, linear calibration curve for glucose detection at 652 nm and selectivity for glucose. Reproduced with permission [66]. Copyright 2019, American Chemical Society. (c) Schematic of 2D-MOFs-nanozyme sensor arrays probing phosphates and their related hydrolytic processes and 2D canonical score plot for the first two factors of the colorimetric-response patterns obtained against 10 μmol/L phosphates. Reproduced with permission [67]. Copyright 2018, American Chemical Society. (d) Schematic illustration of PSMOF as an oxidase mimic for cellular glutathione detection, UV–vis absorption spectra of PSMOF-oxidized TMB in the absence and presence of GSH at different concentrations (0–40 μmol/L), selectivity of the PSMOF sensor for GSH and GSH detection in Hela and LO2 cells. Reproduced with permission [69]. Copyright 2019, American Chemical Society.

catalytic activity was developed for cancer cells detection [64]. The surface of Ni-hemin MOFs was modified with folic acid, a targeting ligand for cancer cells. The selective binding Ni-hemin MOFs cause significant color change by oxidation of TMB in the presence H_2O_2. The LOD can be achieved as 10 cells/mL for MCF-7. Lin's group synthesized a superior nanozyme with enriched 2D catalytic interface, which was composed of Fe-MOFs and GO (Fig. 5a) [65]. The amplified peroxidase-like catalytic ability was applied for ultrasensitive detection of typical biomarker of woodsmoke exposure in human blood. The LOD was as low as 0.268 ng/mL. Fe-MIL-88B-NH_2 immobilizing glucose oxidase (GOx) *via* an amidation coupling reaction was utilized to perform a cascade catalysis for the colorimetric detection of glucose (Fig. 5b) [66]. The "nanoscale proximity effects" diminished the effect of diffusion resistance and decomposition of H_2O_2. As a result, the glucose biosensors showed strong temperature adaptation and acid-base tolerance with a LOD of 0.478 μmol/L. Wei's group fabricated sensor arrays constructed by three 2D-MOFs nanozymes for detection and discrimination of phosphates as well as monitoring the phosphate-related enzymatic hydrolytic processes (Fig. 5c) [67]. Pyrophosphate (PPi), adenosine triphosphate (ATP), and adenosine diphosphate (ADP) would inhibit the peroxidase-like activity of the 2D-MOFs, while their hydrolytic product, phosphate (Pi), exhibited no such inhibitory ability. Based on this principle, a simple colorimetric method with tunable dynamic range for alkaline phosphatase (ALP) activity assay was developed by integrating with ALP catalyzed hydrolytic reaction [68]. Moreover, Wei's group developed a photosensitized metal-organic framework (PSMOF) with excellent oxidase-like activity as colorimetric probe for cellular GSH detection (Fig. 5d) [69]. A derivative of $Ru(bpy)_3^{2+}$ with stronger visible-light absorption was used as PS linker. The oxidase-like activity of PSMOF could be modulated by switching light on and off. On the basis of efficient inhibition of GSH toward PSMOF catalysis, the PSMOF was applied as a functional colorimetric probe for GSH detection with LOD of ~0.68 μmol/L. In general, it is proven that the nMOFs-based nanozymes are promising to be used for detection of biomarkers and early diagnosis with reliablity.

3.2. NMOFs as enzyme carriers

In addition, nMOFs without enzyme-like activity could act as excellent enzyme carrier due to the high loading capacity. Enzyme molecules were protected from biological, thermal and chemical degradation by nMOFs, while the biological activity was maintained. For example, NiPd hollow nanoparticles and GOx were simultaneously immobilized on ZIF-8 through co-precipitation method as a colorimetric sensor for glucose detection [70]. The prepared GOx@ZIF-8(NiPd) nanoflowers showed the peroxidase-like activity of NiPd hollow nanoparticles and maintained the enzyme activity of GOx as well, realizing the cascaded sensor for visual detection. A novel colorimetric sensor for antibiotics was developed through embedding horseradish peroxidise (HRP) into zeolitic metal azolate framework-7 (MAF-7), which could not only prevent HRP aggregation but also enhance HRP activity [71]. Con-

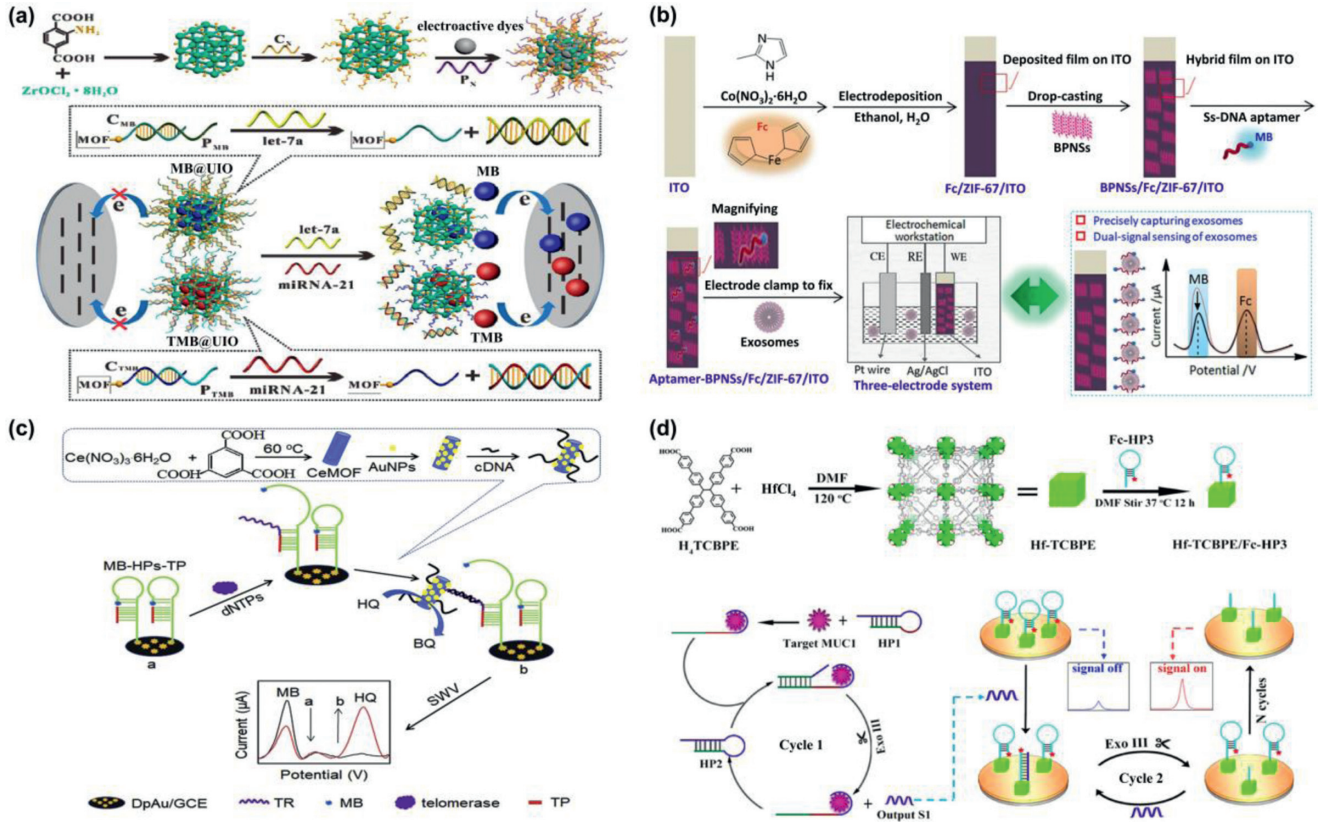

Fig. 6. (a) Schematic representation of nucleic acid-functionalized MOFs fabrication procedure and the principle of the MOF-based homogeneous electrochemical biosensor for multiple detection of miRNAs. Reproduced with permission [73]. Copyright 2019, American Chemical Society. (b) Diagram of the construction process and application of a dual-signal and intrinsic self-calibration aptasensor of exosomes. Reproduced with permission [77]. Copyright 2020, American Chemical Society. (c) Schematic illustration of the ratiometric electrochemical strategy based on catalysis of Au@CeMOF toward HQ oxidation and conformation switch of MB labeled hairpin DNA for detection of telomerase activity. Reproduced with permission [79]. Copyright 2019, Elsevier B.V. (d) Synthesis of Hf-MOF, Exo III-assisted recycling amplification strategy and construction of the ECL sensor. Reproduced with permission [81]. Copyright 2020, American Chemical Society.

sequently, a significant color signal can be observed with high sensitivity and low LOD of 0.51 pg/mL.

All the above-mentioned nMOFs displayed the significant property tunability as well as protection, which served a space for designing of colorimetric biosensors. The biomarkers can be detected through affecting the catalytic activity of nMOFs-based nanozymes or combining with other functional molecules and analytic technique.

4. Electrochemical sensing

Through collecting and analyzing the electrical signal originated from electrochemical reactions, electrochemistry can be used to qualitative or quantitative detection of target analytes. Owing to the fascinating superiorities such as simple operation, rapidity, high sensitivity, and low cost, electrochemical sensing has attracted widespread attention [72].

4.1. NMOFs as nanocontainer

Although most of nMOFs cannot be used directly for electrocatalysis due to the poor conductivity, introducing nMOFs into electrochemical system still has many advantages. On one hand, the high porosity of nMOFs will increase the loading rate of electroactive substances. On the other hand, nMOFs are able to maintain stability of active substances and avoid the interference from external environments. For instance, UIO-66-NH_2 was used as nanocontainer loading with electroactive dyes for miRNA detection (Fig. 6a) [73]. DsDNA acted as gatekeepers to cap MOFs and were separated from MOFs when formed the RNA-DNA complexes with target miRNA. The electrochemical signals of dyes released from UIO-66-NH_2 were collected and simultaneous detection of let-7a and miRNA-21 was achieved, with LOD down to 3.6 and 8.2 fmol/L, respectively. In the electrochemical nitrite sensing platform based on AuNPs decorated Cu-MOF, Cu-MOF could increase the adsorption capacity of nitrite and prevent the aggregation of AuNPs in the electrodeposition process. Consequently, the electrochemical sensing platform demonstrated LOD of 82 nmol/L for the detection of nitrite [74]. It is interesting that the crystalline morphology of nMOFs as supporting materials might influence the detection performance of electrochemical sensors [75].

Besides, introduction of aptamers to recognize biomarkers with highly specificity is an effective strategy for detection and diagnosis as well. In aptamer-nMOFs-based biosensors, nMOFs would facilitate aptamer strand immobilization [76]. Through electrochemical impedance spectroscopy and differential pulse voltammetry, the electrochemical aptasensor displayed good sensing performances. After that, a novel dual-signal and intrinsic self-calibration aptasensor was developed for detection of exosomes. Ferrocene (Fc)-doped ZIF-67 was assembled on indium tin oxide (ITO) slice, followed by combining methylene blue (MB)-labeled ssDNA aptamer (Fig. 6b) [77]. In the presence of specific exosomes, the redox current of MB regularly reduced and that of Fc (as reference) rarely changed. This novel aptasensor could efficiently detect exosomes in the concentration range from 1.3×10^2 particles/mL to 2.6×10^5 particles/mL, with a low LOD of 100 particles/mL. From

these works, it is observed that nMOFs were used as containers of electroactive dyes or supporter for modification of functional molecules, contributing to the generation and transformation of electrochemical signals.

4.2. NMOFs with electrocatalytic activity

Compared with bulk nMOFs, 2D nMOFs could present superior sensing performance owing to the decreased contact resistance and enhanced charge transfer rate at the interface between the electrode and the electrolyte. To date, some nMOFs display satisfactory electrocatalytic activity and corresponding electrochemical signals. For example, a hierarchical sheet-like Ni-BDC MOF with superior electrocatalytic oxidation toward glucose sensing was demonstrated [78]. Compared with bulk Ni-BDC, sheet-like Ni-BDC indicated better glucose sensing performance (with low LOD of 6.68 μmol/L) owing to the good electric conductivity as well as more accessible active sites and diffusion interspaces. Furthermore, using two independent electrochemical signal peaks, a telomerase ratiometric electrochemical biosensor has been developed (Fig. 6c) [79]. The Au@CeMOF tags demonstrated an excellent electrocatalysis toward hydroquinone (HQ) oxidation to *p*-benzoquinone (BQ). Meanwhile, a MB labeled hairpin DNA was immobilized on the electrode surface *via* Au-S bond. After conformational switch of hairpin DNA, a ratiometric signal (I_{BQ}/I_{MB}) was recorded for electrochemical detection of telomerase activity, showing wide dynamic correlation of telomerase activity from 2×10^2 cells/mL to 2×10^6 cells/mL with LOD of 27 cells/mL.

Electrochemiluminescence resonance energy transfer (ECLRET) has been used to design biosensors with favorable features including high sensitivity, non-selective light excitation and inexpensive instruments. According to luminescence resonance energy transfer (LRET) mechanism, ECLRET is caused by energy transfer from donor to acceptor. A MOFs-based ECL RNA sensing platform was established, in which Fe-MIL-88 MOFs not only acted as an ECL acceptor in ECLRET but also offered metal active centers to consume co-reactant, initiating double quenching effect on the ECL [80]. In presence of target RNA, the specific cleavage *via* endonuclease IV was permitted to release the nanotag and the ECL signal was turned on. In another example, matrix coordination-induced ECL (MCI-ECL) enhancement was discovered in case of Hf-MOF (Fig. 6d) [81]. Considering the unique characteristic, a new ECL indicator consisted of Hf-MOF and phosphate-terminal ferrocene-labeled hairpin DNA aptamer was employed to construct a novel "off-on" ECL sensor. With the assistance of the exonuclease III (Exo III)-assisted recycling amplification strategy, the ECL sensor displayed ultrasensitive detection ability toward mucin 1 (MUC1) with linear response range from 1 fg/mL to 1 ng/mL and LOD of 0.49 fg/mL.

Based on the above approaches of nMOFs-based electrochemical biosensors, sensitive detections of unique biomarkers were realized through this simple and convenient analytical approach. It would be a highly potential solution for accurate detection of biomarkers for early diagnosis after determining and designing the function and property of nMOFs.

5. SERS sensing

SERS technology, as one of the most promising detection methods in recent years, is developed on the basis of the Raman scattering phenomenon discovered by scientists Raman [82]. Owing to the rich fingerprint, anti-photobleaching and anti-photodegradation, non-invasive and other characteristics, SERS has been widely used to detect biomolecules with ultra-high detection sensitivity [83–85].

5.1. NMOFs for pre-concentrating and protection

SERS is mainly caused by the electromagnetic enhancement (EM) effect originated from localized surface plasmon resonance (LSPR) of precious metal nanoparticles such as Au, Ag and Cu [86,87]. NMOFs with strong adsorption capability have been used for pre-concentrating of analytes and further enhancing the SERS signal. For example, gaseous molecules are difficult to be detected owing to their much faster diffuse rates compared to liquid or solid molecules. By assembling ZIF-8 on the surface of gold superparticles (GSPs), the diffusion of 4-ethylbenzaldehyde (a volatile organic compound (VOC) and a biomarker for lung cancer) was obviously slowed (Fig. 7a) [88]. As a result, large quantities of 4-ethylbenzaldehyde molecules were enriched within nMOFs. Simultaneously, ZIF-8 shell could suppress the exponential decay of the electromagnetic field around the GSP to improve the SERS detection signal. *Via* a Schiff base reaction with *p*-aminothiophenol (4-ATP) modified on the surface of GSP, 4-ethylbenzaldehyde was detected using the I_{1623}/I_{1078} SERS signal ratio with a LOD of 10 ppb. The proposed strategy for gaseous molecules detection is of great significance for early lung cancer diagnosis. Besides, a plasmonic nose based on a ZIF-8-encapsulated Ag nanocube array was designed for ultratrace recognition of VOC vapor [89]. Through optimizing the effective preconcentration of gas and intensifying electromagnetic hotspots between adjacent Ag nanocubes, the plasmonic nose enabled in-situ detection of adsorption kinetics and recognition of various VOCs with LOD down to ppb levels. Combining the advantages of Raman spectroscopy and remote detection, the Ag@MOF core-shell SERS platform realized real-time and stand-off VOCs monitoring (Fig. 7b) [90]. Recently, a novel method for fabrication of Au@MOF core-shell structure was developed at room temperature [91]. This simple and convenient synthesis method provides a broader prospect for MOF-based SERS substrates with high-performance.

Apart from pre-concentrating, nMOFs can also prevent metal nanoparticles from agglomerating as well [92]. Wei's group designed a SERS active substrate by *in situ* growing AuNPs into porous MIL-101 for detection of glucose and lactate (Fig. 7c) [93]. MIL-101 could prevent AuNPs from aggregation especially in complex biological samples to ensure the perfect catalytic activity. The obtained AuNPs@MIL-101, acting as peroxidase mimics, oxidized the Raman-inactive reporter leucomalachite green (LMG) into Raman-active malachite green (MG) in presence of H_2O_2. Simultaneously, AuNPs@MIL-101 acted as the SERS substrates to enhance the Raman signals of as-produced MG. The efficient enzymatic cascade reactions were enabled for facile SERS bioassays after assembling oxidases onto AuNPs@MIL-101, realizing the real-time monitoring of glucose and lactate with good sensitivity and selectivity. Recently, a bioenzyme-free SERS assay platform for glucose detection was constructed by *in-situ* modifying AuNPs onto 2D Cu-TCPP(Fe) nanosheets based on cascade catalysis reactions [94]. The MOF nanosheets uniformly loaded AuNPs and effectively prevented the agglomeration, providing more active sites for the enzyme-like catalytic reactions. At the same time, the AuNPs were beneficial to the enhancement of Raman signals of probe molecules, realizing the quantitative detection of glucose with the LOD of 3.9 μmol/L. For real samples, identifications of unknown components are extremely difficult because of complicated SERS signals induced by non-selective enrichment. The MOFs shell could play an analyte filtration function to improve the identification ability [95].

5.2. NMOFs as SERS-active substrate

Impressively, high-intensity SERS signals can be directly obtained from nMOFs thanks to the inherent chemical enhancement

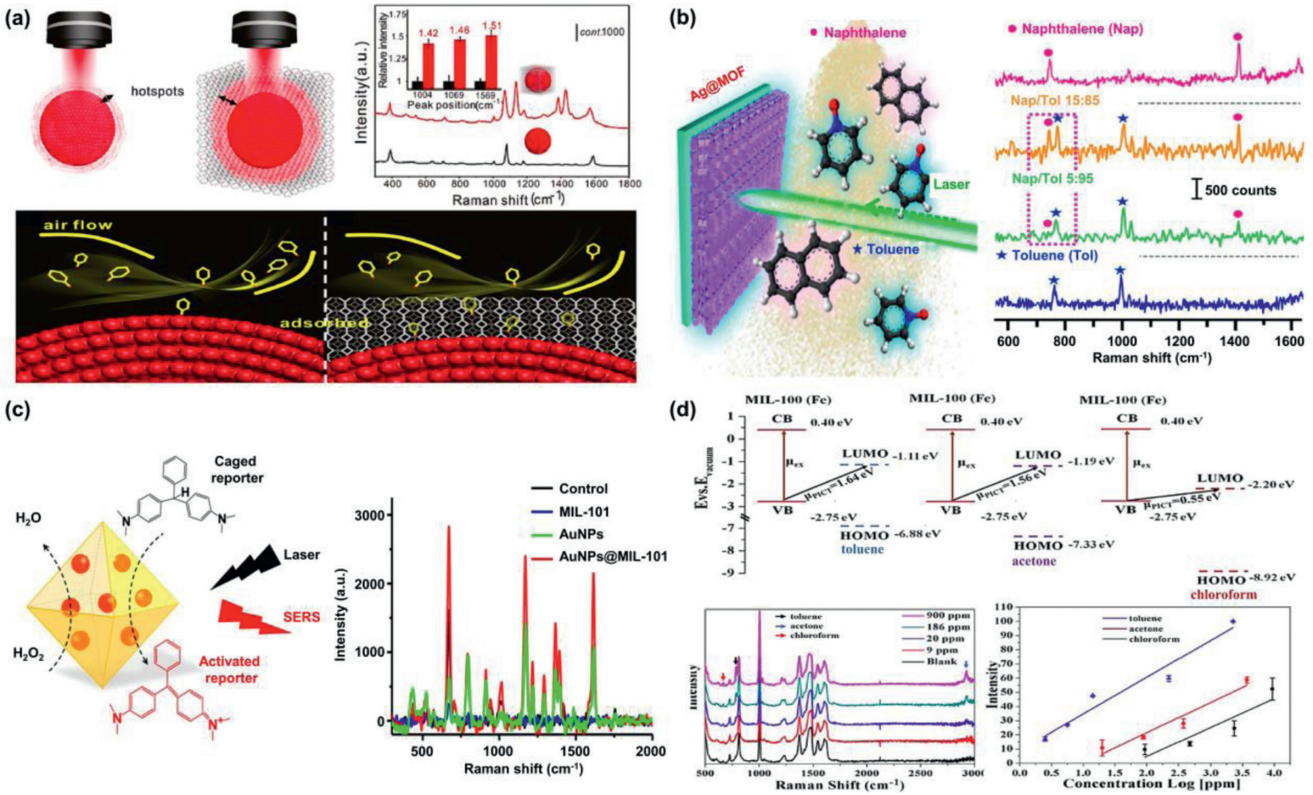

Fig. 7. (a) Hotspots in GSPs (left) and GSPs@ZIF-8 (right) around the edges of the plasmon, SERS spectra of 4-ATP and on GSPs (black) and GSPs@ZIF-8 (red) (inset: relative intensity) and schematic illustration of gas collisions. Reproduced with permission [88]. Copyright 2017, WILEY-VCH Verlag GmbH & Co. KGaA, Weinheim. (b) Scheme showing the stand-off detection of aerosolized toluene and naphthalene, and stand-off multiplex SERS spectra. Reproduced with permission [90]. Copyright 2019, American Chemical Society. (c) Schematic illustration of AuNPs@MIL-101 acting not only as the peroxidase mimics but also as the SERS substrates and corresponding SERS spectra of different samples containing LMG and H_2O_2. Reproduced with permission [93]. Copyright 2017, American Chemical Society. (d) Energy-level diagrams of three different VOCs to MIL-100 (Fe) (*vs.* vacuum), SERS spectra of multiplex sensing for VOCs and semi-log plots of Raman intensity as a function of VOCs concentrations. Reproduced with permission [97]. Copyright 2020, Wiley-VCH GmbH.

property. The chemical enhancement mechanism is associated with charge transfer (CT) between adsorbed molecules and substrates. The electronic energy band of nMOFs could be purposely adjusted to match the target analytes by altering the metal center, organic ligands and skeleton topology and the enhancement factor (EF) of this SERS detection method without "hot spots" would be increased to 10^6 [96]. Lately, MIL-100(Fe) as an excellent SERS-active substrate with high sensitivity and EF of 10^5 was demonstrated for multiplex detection of VOCs (Fig. 7d) [97]. The high SERS activity of MIL-100(Fe) substrate originated from CT enhancement mechanism. When combined with AuNPs, CT and EM resulted in different signal enhancements and the platform of MIL-100(Fe) with Au deposition provided remarkable EF up to 10^{10} and a LOD down to 0.48 ppb. These CT enhancements can be adequately considered as a new venue for the development of SERS-active nMOFs biosensors, which is especially for selective detection toward specific analytes.

From the researches of nMOFs-based SERS platforms for unlabeled-detection, it turned out that nMOFs are not only beneficial to the enrichment of analytes but also responsible for the stability of nanoparticles. As a result, the biomolecules especially gaseous biomarkers are detected with improved sensitivity thanks to the EM and CT enhancement.

6. Conclusion and outlook

In this review, the rapid advancements of nMOFs for biosensing in recent years have been carefully introduced. We discussed the development of nMOFs biosensors detection of biomarker and early diagnosis with four different sensing strategies. Firstly, popular fluorescence sensing was introduced. Based on the advantage of controllable functions and properties, nMOFs could be designed as fluorophores, quenchers or skeletons for loading fluorophore. Although labeled molecules are needed, nMOFs as fluorescent nanoprobes exhibit good molecular recognition and signal transduction, realizing the rapid or even real-time detection of biomarkers. Secondly, a convenient method, colorimetric sensing, was presented. Thanks to the inherent enzyme-like catalytic activity of certain nMOFs or excellent protection effect for natural enzyme, the biomarkers can be detected by naked eye or common apparatus. With the aid of chromogenic substrate, biomimetic catalysis provided a rapid and inexpensive strategy for diagnostic applications. Thirdly, electrochemistry sensing with rapid response and high sensitivity was demonstrated. Despite the electrochemical signals are sensitive with changes of conditions, the porous nMOFs not only avoid the interference from the external environment but also increase the loading rate of electroactive substances. It would be a highly potential solution for accurate detection of biomarkers for early diagnosis, but improving the conductivity is critically vital as well. Finally, one of most promising detection methods, SERS sensing, was described. Owing to the excellent enhancement effect of noble metal nanoparticles or the nMOFs itself, biomarkers would be pre-concentrated and label-free recognized with ultra-high detection sensitivity. Combining with the adsorption ability of nMOFs, the SERS sensing is enormously suitable for gaseous biomarkers, which is rare to achieve for other sensing modes. As an

emerging technology, further significant developments in biomarkers detection are still needed. As can be seen above, for a variety of analytical techniques, nMOFs play constructive roles owing to the designable functions and properties. Furthermore, the porosity of nMOFs can also be utilized to assist the detection process. In order to develop biosensors with both higher sensitivity and selectivity, the various sensing platforms would be encouraged to combine with other mature or rising principles/technologies, such as aggregation induced emission (AIE), ELISA, specific host-guest interactions, microfluidic, HCR and recycling amplification strategy.

Despite nMOFs have been widely used in various analytic strategy, there are still many more efforts that need to be devoted to realize the full potential of nMOFs biosensors. First, since biosensing is usually carried out in biological mediums, enhancing the water stability of nMOFs is a prerequisite to avoid the aggregation and framework breakdown during the detection process. From this, the analytic results can be credible and repeatable. Second, improving the reusability of nMOFs biosensors. NMOFs combining with magnetic materials could be separated easily after detection to recycle. Furthermore, coupling with structural simulations and theoretical models so that the correlation between structure and performance will be better understood to guide the design process and improve the functionalization efficiency. In addition, developing more portable devices and convenient operation is demanded for *in situ* and practical applications. Lastly, for *in vivo* sensing, the biocompatibility and toxicity need to be considered. The accumulation and decomposition of nMOFs *in vivo* may cause potential biological toxicity. Up to now, toxicity results dealing with nMOFs are limited. It is necessary to comprehensive assessment of various nMOFs' acute and long-term toxicity data.

In conclusion, nMOFs biosensors have attracted attentions owing to their excellent performances and have provided an incredible opportunity in the biomedical field especially detection of biomarker and early diagnosis. How to use nMOFs to design multifunctional biologic nano-platforms remains innovative prospects. In the subsequent researches, the points should not only focus on the development of new functional nMOFs, but also solve their clinical application challenges. It is expected that nMOFs will play a better role in the diagnosis of clinical diseases.

Declaration of competing interest

There is no conflict of interest to report.

Acknowledgments

This work was supported by grants from the National Natural Science Foundation of China (Nos. 22022412, 21874155), the Natural Science Foundation of Jiangsu Province (No. BK20191316), and the Qing-Lan Project of Jiangsu Province (2019).

References

[1] R. Gui, H. Jin, X. Bu, et al., Coord. Chem. Rev. 383 (2019) 82–103.
[2] D. Yue, M. Wang, F. Deng, et al., Chin. Chem. Lett. 29 (2018) 648–656.
[3] A. Chen, S. Yang, Biosens. Bioelectron. 71 (2015) 230–242.
[4] G.A. Santiago, J. Vázquez, S. Courtney, et al., Nat. Commun. 9 (2018) 1391.
[5] Y. Xiong, Y. Leng, X. Li, X. Huang, Y. Xiong, TrAC Trends Anal. Chem. 126 (2020) 115861.
[6] J. Kim, A.S. Campbell, B.E.F. de Ávila, J. Wang, Nat. Biotechnol. 37 (2019) 389–406.
[7] Y. Li, X. Liu, X. Xu, et al., Adv. Funct. Mater. 29 (2019) 1905568.
[8] L. Wu, H. Ding, X. Qu, et al., J. Am. Chem. Soc. 142 (2020) 4800–4806.
[9] V.T. Nguyen, Y.S. Kwon, M.B. Gu, Curr. Opin. Biotechnol. 45 (2017) 15–23.
[10] A. Smart, A. Crew, R. Pemberton, et al., TrAC Trends Anal. Chem. 127 (2020) 115898.
[11] Q. Zhou, D. Tang, Trends Anal. Chem. 124 (2020) 115814.
[12] E. Skaria, B.A. Patel, M.S. Flint, K.W. Ng, Anal. Chem. 91 (2019) 4436–4443.
[13] C. Ji, Y. Zhou, R.M. Leblanc, Z. Peng, ACS Sens. 5 (2020) 2724–2741.
[14] B. Liu, Y. Zhao, Y. Jia, J. Liu, J. Am. Chem. Soc. 142 (2020) 14702–14709.
[15] V. Yadav, S. Roy, P. Singh, Z. Khan, A. Jaiswal, Small 15 (2019) 1803706.
[16] C. Wang, X.P. Zhao, F.F. Liu, et al., Nano Lett. 20 (2020) 1846–1854.
[17] K. Wang, L. Jiang, F. Zhang, et al., Anal. Chem. 90 (2018) 14056–14062.
[18] K. Wang, L. Shangguan, Y. Liu, et al., Anal. Chem. 89 (2017) 7262–7268.
[19] Y. Li, Y. Ma, X. Jiao, et al., Nat. Commun. 10 (2019) 1036.
[20] J. Cao, X.P. Zhao, M.R. Younis, et al., Anal. Chem. 89 (2017) 10957–10964.
[21] J. Yu, P. Luo, C. Xin, et al., Anal. Chem. 86 (2014) 8129–8135.
[22] J. Yu, L. Zhang, X. Xu, S. Liu, Anal. Chem. 86 (2014) 10741–10748.
[23] N. Zhang, L. Yan, Y. Lu, et al., Chin. Chem. Lett. 31 (2020) 2071–2076.
[24] S. Zhang, X. Pei, H. Gao, S. Chen, J. Wang, Chin. Chem. Lett. 31 (2020) 1060–1070.
[25] S. Lv, K. Zhang, L. Zhu, D. Tang, Anal. Chem. 92 (2020) 1470–1476.
[26] H.C. Zhou, J.R. Long, O.M. Yaghi, Chem. Rev. 112 (2012) 673–674.
[27] X.Y. Li, Y.Z. Li, L.N. Ma, et al., J. Mater. Chem. A 8 (2020) 5227–5233.
[28] Y. Feng, P. Dong, L. Cao, et al., J. Mater. Chem. A 9 (2021) 2135–2144.
[29] L. Chong, J. Wen, J. Kubal, et al., Science 362 (2018) 1276–1281.
[30] C. Wang, F.F. Liu, Z. Tan, et al., Adv. Funct. Mater. 30 (2020) 1908804.
[31] F.F. Liu, Y.C. Guo, W. Wang, Y.M. Chen, C. Wang, Nanoscale 12 (2020) 11899–11907.
[32] W.C. Hu, Y. Shi, Y. Zhou, et al., J. Mater. Chem. A 7 (2019) 10601–10609.
[33] M. Yoon, R. Srirambalaji, K. Kim, Chem. Rev. 112 (2012) 1196–1231.
[34] I. Stassen, N. Burtch, A. Talin, et al., Chem. Soc. Rev. 46 (2017) 3185–3241.
[35] K. Zhang, K. Dai, R. Bai, et al., Chin. Chem. Lett. 30 (2019) 664–667.
[36] M. Wang, L. Guo, D. Cao, Anal. Chem. 90 (2018) 3608–3614.
[37] L. Hou, Y. Qin, J. Li, et al., Biosens. Bioelectron. 143 (2019) 111605.
[38] D. Yan, Y. Lou, Y. Yang, et al., ACS Appl. Mater. Interfaces 11 (2019) 47253–47258.
[39] S. Wu, H. Min, W. Shi, P. Cheng, Adv. Mater. 32 (2020) 1805871.
[40] X. Wang, W. Fan, M. Zhang, et al., Chin. Chem. Lett. 30 (2019) 801–805.
[41] A. Afzalinia, M. Mirzaee, ACS Appl. Mater. Interfaces 12 (2020) 16076–16087.
[42] L. Chang, X.Y. Yao, Q. Liu, et al., Talanta 183 (2018) 83–88 183.
[43] L. Guo, M. Wang, D. Cao, Small 14 (2018) 1703822.
[44] D. Yue, D. Zhao, J. Zhang, et al., Chem. Commun. 53 (2017) 11221–11224.
[45] D. Wu, Z. Zhang, X. Chen, et al., Chem. Commun. 55 (2019) 14918–14921.
[46] A. Sousaraei, C. Queirós, F.G. Moscoso, et al., Anal. Chem. 91 (2019) 15853–15859.
[47] Y. Wang, Q. Liu, Q. Zhang, B. Peng, H. Deng, Angew. Chem. Int. Ed. 57 (2018) 7120–7125.
[48] H. Chen, J. Wang, D. Shan, et al., Anal. Chem. 90 (2018) 7056–7063.
[49] M. Zhao, Y. Wang, Q. Ma, et al., Adv. Mater. 27 (2015) 7372–7378.
[50] W.J. Song, Talanta 170 (2017) 74–80.
[51] Q. Yang, J. Hong, Y.X. Wu, et al., ACS Appl. Mater. Interfaces 11 (2019) 41506–41515.
[52] H.S. Wang, H.L. Liu, K. Wang, et al., Anal. Chem. 89 (2017) 11366–11371.
[53] H.S. Wang, J. Li, J.Y. Li, et al., NPG Asia Mater. 9 (2017) 354.
[54] X. Huang, Z. He, D. Guo, et al., Theranostics 8 (2018) 3461–3473.
[55] Y.B. Hao, Z.S. Shao, C. Cheng, et al., ACS Appl. Mater. Interfaces 11 (2019) 31755–31762.
[56] P. Ling, C. Qian, J. Yu, F. Gao, Chem. Commun. 55 (2019) 6385–6388.
[57] W. Zhang, X. Liu, P. Li, et al., Anal. Chem. 92 (2020) 3716–3721.
[58] S. Wu, C. Li, H. Shi, Y. Huang, G. Li, Anal. Chem. 90 (2018) 9929–9935.
[59] X. Meng, K. Zhang, F. Yang, et al., Anal. Chem. 92 (2020) 8333–8339.
[60] J. Zhang, M. He, C. Nie, et al., Anal. Chem. 91 (2019) 9049–9057.
[61] C. Yang, K. Chen, M. Chen, et al., Anal. Chem. 91 (2019) 2727–2733.
[62] L. Feng, M. Liu, H. Liu, et al., ACS Appl. Mater. Interfaces 10 (2018) 23647–23656.
[63] S. Li, X. Liu, H. Chai, Y. Huang, Trends Anal. Chem. 105 (2018) 391–403.
[64] N. Alizadeh, A. Salimi, R. Hallaj, F. Fathi, F. Soleimani, J. Nanobiotechnol. 16 (2018) 93.
[65] X. Ruan, D. Liu, X. Niu, et al., Anal. Chem. 91 (2019) 13847–13854.
[66] W. Xu, L. Jiao, H. Yan, et al., ACS Appl. Mater. Interfaces 11 (2019) 22096–22101.
[67] L. Qin, X. Wang, Y. Liu, H. Wei, Anal. Chem. 90 (2018) 9983–9989.
[68] X. Wang, X. Jiang, H. Wei, J. Mater. Chem. B 8 (2020) 6905–6911.
[69] Y. Liu, M. Zhou, W. Cao, et al., Anal. Chem. 91 (2019) 8170–8175.
[70] Q. Wang, X. Zhang, L. Huang, Z. Zhang, S. Dong, Angew. Chem. Int. Ed. 56 (2017) 16082–16085.
[71] L. Wang, G. Liu, Y. Ren, et al., Anal. Chem. 92 (2020) 14259–14266.
[72] X. Zhang, G. Li, D. Wu, et al., Biosens. Bioelectron. 137 (2019) 178–198.
[73] J. Chang, X. Wang, J. Wang, H. Li, F. Li, Anal. Chem. 91 (2019) 3604–3610.
[74] H. Chen, T. Yang, F. Liu, W. Li, Sens. Actuators B: Chem. 286 (2019) 401–407.
[75] D. Sun, D. Yang, P. Wei, et al., ACS Appl. Mater. Interfaces 12 (2020) 41960–41968.
[76] N. Zhou, F. Su, C. Guo, et al., Biosens. Bioelectron. 123 (2019) 51–58.
[77] Y. Sun, H. Jin, X. Jiang, R. Gui, Anal. Chem. 92 (2020) 2866–2875.
[78] G. Gumilar, Y.V. Kaneti, J. Henzie, et al., Chem. Sci. 11 (2020) 3644–3655.
[79] P. Dong, L. Zhu, J. Huang, J. Ren, J. Lei, Biosens. Bioelectron. 138 (2019) 111313.
[80] Y.W. Zhang, W.S. Liu, J.S. Chen, et al., Sens. Actuators B: Chem. 321 (2020) 128456.
[81] W. Huang, G.B. Hu, L.Y. Yao, et al., Anal. Chem. 92 (2020) 3380–3387.
[82] C.V. Raman, Nature 121 (1928) 619.
[83] K. Cui, C. Fan, G. Chen, et al., Anal. Chem. 90 (2018) 12137–12144.
[84] G. Qi, H. Li, Y. Zhang, et al., Anal. Chem. 91 (2019) 1408–1415.
[85] S. Tian, O. Neumann, M.J. McClain, et al., Nano Lett. 17 (2017) 5071–5077.
[86] S.Y. Ding, J. Yi, J.F. Li, et al., Nat. Rev. Mater. 1 (2016) 16021.
[87] S.Y. Ding, E.M. You, Z.Q. Tian, M. Moskovits, Chem. Soc. Rev. 46 (2017) 4042–4076.

[88] X. Qiao, B. Su, C. Liu, et al., Adv. Mater. 30 (2018) 1702275.
[89] C.S.L. Koh, H.K. Lee, X. Han, H.Y.F. Sim, X.Y. Ling, Chem. Commun. 54 (2018) 2546–2549.
[90] G.C. Phan-Quang, N. Yang, H.K. Lee, et al., ACS Nano 13 (2019) 12090–12099.
[91] J.W.M. Osterrieth, D. Wright, H. Noh, et al., J. Am. Chem. Soc. 141 (2019) 3893–3900.
[92] W.C. Hu, M.R. Younis, Y. Zhou, C. Wang, X.H. Xia, Small 16 (2020) 2000553.
[93] Y. Hu, H. Cheng, X. Zhao, et al., ACS Nano 11 (2017) 5558–5566.
[94] S. Hu, Y. Jiang, Y. Wu, et al., ACS Appl. Mater. Interfaces 12 (2020) 55324–55330.
[95] Q. Ding, J. Wang, X. Chen, et al., Nano Lett. 20 (2020) 7304–7312.
[96] H. Sun, S. Cong, Z. Zheng, et al., J. Am. Chem. Soc. 141 (2019) 870–878.
[97] J.H. Fu, Z. Zhong, D. Xie, et al., Angew. Chem. Int. Ed. 59 (2020) 20489–20498.